

Kinetic analysis of superoxide anion radical- and hydroxyl radical-scavenging activities of platinum nanoparticles.

*Takeki Hamasaki[†], Taichi Kashiwagi[†], Toshifumi Imada[†], Noboru Nakamichi[‡], Shinsuke Aramaki[†],
Kazuko Toh[†] □ Shinkatsu Morisawa[‡], Hisashi Shimakoshi[§], Yoshio Hisaeda[§], and Sanetaka
Shirahata^{*†}*

[†]Department of Genetic Resources Technology, Faculty of Agriculture, Kyushu University,
Hakozaki, Higashi-ku, Fukuoka 812-8581, Japan

[‡]Nihon Trim Co. Ltd., 1-8-34 Oyodonaka, Kita-ku, Osaka 531-0076, Japan

[§]Department of Chemistry and Biochemistry, Graduate School of Engineering, Kyushu University,
Hakozaki, Higashi-ku, Fukuoka 812-8581, Japan

Supporting data

1.1. Determination of the second order rate constant for analysis of superoxide anion ($O_2^{\cdot-}$) and platinum nanoparticles (Pt nps). To determine the rate of reaction of Pt nps with $O_2^{\cdot-}$, a kinetic model for the ESR analysis reported earlier was adopted for the reactions of various antioxidants with the superoxide anion^{1,2}. According to this model, the concentration of $O_2^{\cdot-}$, $[O_2^{\cdot-}]$ can be described as follows:

$$d[O_2^{\cdot-}]/dt = k_{SA}[XOD][HPX] - k_{DMPO}[DMPO][O_2^{\cdot-}] - k_S[S]^f[O_2^{\cdot-}], \quad (1)$$

where $[XOD]$, $[HPX]$, $[DMPO]$ and $[S]$ represent the concentrations of XOD, HPX, DMPO and scavenger, respectively. k_{DMPO} , k_S and k_{SA} are second-order rate constants for the three reactions and f

represents an apparent molecule number of scavenger or an active site which reacts with one molecule of $O_2^{\cdot-}$. In this system, spontaneous background dismutation also occurs, as follows:



Equation (2) can be ignored in this experiment as the high concentration of DMPO (0.45 M) traps almost all of the superoxide (Supporting Fig. 1A). Using the steady state approximation ($d[O_2^{\cdot-}]/dt = 0$), equation (1) can be re-written as:

$$k_{SA}[XOD][HPX] - k_{DMPO}[DMPO][O_2^{\cdot-}] - k_S[S]^f[O_2^{\cdot-}] = 0. \quad (3)$$

The velocity of DMPO- $O_2^{\cdot-}$ ($V^{DMPO-O_2^{\cdot-}}$) can be represented by the following equation:

$$d[DMPO-O_2^{\cdot-}]/dt = V^{DMPO-O_2^{\cdot-}} = k_{DMPO}[DMPO][O_2^{\cdot-}]. \quad (4)$$

From equation (4) the concentration of $O_2^{\cdot-}$ can be calculated:

$$[O_2^{\cdot-}] = V^{DMPO-O_2^{\cdot-}}/(k_{DMPO}[DMPO]). \quad (5)$$

The velocity of $O_2^{\cdot-}$ (V^{SA}) is:

$$V^{SA} = k_{SA}[XOD][HPX]. \quad (6)$$

Insert (5) and (6) to (3), and then take a reciprocal number of the new version of (3) which yields equation (7):

$$1/V^{SA} = 1/V^{DMPO-O_2^{\cdot-}} + k_{DMPO}[DMPO]/(k_S V^{DMPO-O_2^{\cdot-}}), \quad (7)$$

Then, the following equation can be derived from (7):

$$V^{DMPO-O_2^{\cdot-}}/V^{SA} - 1 = k_{DMPO}[DMPO]/(k_S[S]^f), \quad (8)$$

where $V^{DMPO-O_2^{\cdot-}}$ and V^{SA} represent the formation rates of DMPO- $O_2^{\cdot-}$ adducts and $O_2^{\cdot-}$ radicals, and k_{DMPO} and k_S represent the rate constants for the reaction of $O_2^{\cdot-}$ with DMPO and with a scavenger, respectively. As V^{SA} can be referred to as the DMPO- $O_2^{\cdot-}$ formation rate in the absence of scavengers,

by setting [scavenger] = 0, equation (7) becomes $V^{SA} = V^{DMPO-O_2^{\cdot-}}$. In the case of 50% inhibition (ID_{50}), $V^{SA} = 1/2 V^{DMPO-O_2^{\cdot-}}$ equation (7) can be simplified to:

$$k_S = k_{DMPO}[DMPO]/(ID_{50})^f. \quad (9)$$

A plot of $(V^{SA}/V^{DMPO-O_2^{\cdot-}} - 1)$ vs. $([scavenger]/[DMPO])$ should give a straight line with an intercept of zero when the f value is one. When evaluating the f value and the ID_{50} , the logarithmic form of equations (7) and (8) are utilized:

$$\log[S] = 1/f \{ \log (V^{SA}/V^{DMPO-O_2^{\cdot-}} - 1) \} + \log ID_{50}. \quad (10)$$

The ID_{50} value calculated from the f value serves as a multiplier of the approximation formula computed from plotting $(V^{SA}/V^{DMPO-O_2^{\cdot-}} - 1)$ vs. $([scavenger]/[DMPO])$. ID_{50} is obtained when $(V^{SA}/V^{DMPO-O_2^{\cdot-}} - 1)$ is equal to one. Since the rate constant, k_{DMPO} , for the reaction of DMPO with $O_2^{\cdot-}$ is known³, an approximate rate constant, k_S , for reaction of Pt nps with $O_2^{\cdot-}$ can be calculated from equation (8) using the ID_{50} value. Thus, k_S can be determined using formulae (8) and (9) using the value of V^{SA} at the time of each parallel experiment in the presence of Pt nps.

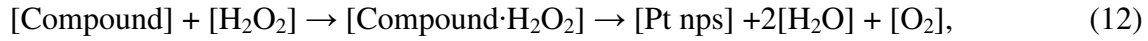
1.2. Hydrogen peroxide-scavenging activity of Pt nps. Pt Nps-catalyst decomposition of hydrogen peroxide was analysed by detecting oxygen production. An YSI Model 5300 Oxygen Monitor (YSI Scientific, Yellow Springs Instrument) with a 5331 Standard Oxygen Probe (Clark electrode) was used to measure the rate of hydrogen peroxide decomposition. The experimental conditions were as follows: The vial was completely filled with the solution and the electrode was inserted into the tightly closed vial. Nitrogen (Nippon Sanso Co., Fukuoka, Japan.) was bubbled through the reaction solution to remove the oxygen. A baseline increase in oxygen concentration of less than 0.5 $\mu\text{M}/\text{min}$ was obtained in the absence of Pt Nps. The reaction solution (4 ml) contained different concentrations of hydrogen peroxide (see figures) in 40 mM sodium phosphate buffer (pH 7.8) at 27 °C. The reaction was initiated by the addition of Pt Nps in oxygen-free water. The concentration of hydrogen peroxide was determined⁴ spectrophotometrically, taking absorbance at

240 nm as $43.6 \text{ M}^{-1}\cdot\text{cm}^{-1}$. The oxygen consumption rate was determined by setting an air-saturated aqueous solution, which contains $243 \text{ }\mu\text{M}$ oxygen at 1 atm and $27 \text{ }^{\circ}\text{C}$, as 100%⁵.

Hydrogen peroxide decomposition by metal particles has already been investigated as one of the simplest catalytic reactions. The decomposition reaction is unimolecular for both Pt nps and catalase, following the chemical equation



The process by which oxygen is generated from hydrogen peroxide by Pt nps (or the active site of Pt nps) can be written as:



where $[\text{Compound}]$ is the concentration of the Pt nps intermediate just before the reaction with hydrogen peroxide to generate oxygen, and $[\text{Compound}\cdot\text{H}_2\text{O}_2]$, $[\text{H}_2\text{O}_2]$, $[\text{Pt nps}]$, $[\text{H}_2\text{O}]$ and $[\text{O}_2]$ are the concentrations of $\text{Compound}\cdot\text{H}_2\text{O}_2$, Pt nps, H_2O and O_2 , respectively. Thus the rate of oxygen production can be written as:

$$d[\text{O}_2]/dt = k_1[\text{Compound}\cdot\text{H}_2\text{O}_2], \quad (13)$$

and the steady state equation is

$$[\text{Pt nanoparticle}]_{\text{Total}} = [\text{Pt nanoparticle}] + [\text{Compound}] + [\text{Compound}\cdot\text{H}_2\text{O}_2], \quad (14)$$

where $[\text{Pt nanoparticle}]_{\text{Total}}$ is the total amount of Pt nps in the system, and

$$K_2 = [\text{Compound}\cdot\text{H}_2\text{O}_2][\text{H}_2\text{O}_2]/[\text{Compound}\cdot\text{H}_2\text{O}_2]. \quad (15)$$

The following equation can be formulated in the steady state:

$$d[\text{O}_2]/dt = k_1[\text{Pt nanoparticle}]_{\text{Total}}[\text{H}_2\text{O}_2]/(K_2 + [\text{H}_2\text{O}_2]). \quad (16)$$

Values of K_2 and k_1 can be obtained from the V_{max} and K_m of the Michaelis-Menten plot and equation (15).

$$V_{max} = k_1 \cdot [\text{Pt nanoparticle}]_{\text{Total}} \text{ and } K_m = K_2. \quad (17)$$

The activity value used is that of a unimolecular reaction with a rate constant k given in $\text{sec}^{-1} \cdot \text{mg}^{-1} \cdot \text{L}$ for hydrogen peroxide decomposition (Supporting Fig. 2A). The reaction can be written as

$$d[\text{H}_2\text{O}_2]/dt = k_2 \cdot [\text{H}_2\text{O}_2]. \quad (18)$$

From formula (17), the equation can be plotted as:

$$\ln\{[\text{H}_2\text{O}_2]_0/[\text{H}_2\text{O}_2]\}/[\text{Pt nps}] = k_3 \cdot t, \quad (19)$$

where $[\text{H}_2\text{O}_2]_0$ and $[\text{Pt nps}]$ are the concentrations of hydrogen peroxide and Pt nps at time zero, and $[\text{H}_2\text{O}_2]$ is the concentration of hydrogen peroxide at time t . The concentration of hydrogen peroxide consumed is twice the concentration of oxygen generated ($[\text{O}_2]_f$).

$$[\text{O}_2]_f = 2[\text{H}_2\text{O}_2]_0 \quad (20)$$

From equations (18) and (19), the reaction constant k_3 can be written as

$$\ln\{[\text{O}_2]_f / [\text{O}_2]\}/[\text{Pt nps}] = k_3 \cdot t \quad (21)$$

This formula was used to calculate the rate constant for the decomposition of hydrogen peroxide by Pt nps.

1.3. Analysis of hydroxyl radical ($\cdot\text{OH}$)-scavenging activities of Pt nps

Experiments to determine the rate constant of the $\cdot\text{OH}$ reaction have been reported previously, using both a Fenton reaction system⁶, and a UV/ H_2O_2 system as an advanced oxidization process (AOP) for attaining the oxidative degradation of organic pollutants⁷. Since the reaction rate could not be examined using the Fenton system, we tried to determine the rate using not only the Fenton reaction, but also UV/ H_2O_2 in the competition reaction with DMPO.

The kinetic competition model of the hydroxyl radical can be rewritten from the model for the $\text{O}_2^{\cdot-}$, by substituting the $\cdot\text{OH}$ for the $\text{O}_2^{\cdot-}$ (k_s to k_s' and $k_{SA} \cdot [\text{XOD}][\text{HPX}]$ to $k_{HR} \cdot [\text{DTPATAC-Fe}^{2+}][\text{H}_2\text{O}_2]$

or $k_{HR} \cdot h\nu[H_2O_2]$). The rate constant value of k_{DMPO} ($3.3 \times 10^9 \text{ M}^{-1}\text{sec}^{-1}$) is used from the reference³. Spontaneous disproportionation of the $\cdot\text{OH}$ also occurs in both systems, but it can be ignored at high (0.15-0.40 M) concentrations of DMPO (Supporting Fig. 4B). Scavenging of the $\cdot\text{OH}$ and inhibition of its generation were studied by changing the trapping rate of hydroxyl radicals with concentrations of DMPO similar to those used in the analysis of superoxide scavenging activity.

Next, we attempted to investigate the enhancement of direct elimination of $\cdot\text{OH}$ by Pt nps in the H_2O_2/UV system. In this system, however, a time-dependent decrease of the DMPO- $\cdot\text{OH}$ signals was observed (Supporting Fig. 4D). Therefore, the following equation was used for calculating the DMPO- $\cdot\text{OH}$ signal intensity at time 0:

$$\ln[\text{DMPO-}\cdot\text{OH}] = \ln[\text{DMPO-}\cdot\text{OH}]_0 - k_4 t, \quad (22)$$

where $[\text{DMPO-}\cdot\text{OH}]_0$ is the initial concentration of DMPO- $\cdot\text{OH}$, k_4 is the pseudo-first-order rate constant and t is the time (sec).

1.4. Determination of a second order rate constant for dissolved oxygen (O_2) and ascorbic acid (AsA).

Second-order kinetics of autoxidation were analyzed by determining the level of dissolved oxygen. Consumption of dissolved O_2 by AsA can be described as follows:

$$-d[O_2]/dt = k_4[\text{AsA}][O_2], \quad (23)$$

where k_4 is the second-order rate constant for O_2 with AsA, and $[\text{AsA}]$ and $[O_2]$ are the concentrations of AsA and O_2 , respectively. The first-order rate constant (k_5) was determined in the presence of a large excess of ascorbic acid (AsA) relative to the amount of dissolved oxygen so that the reaction behaves as a first-order reaction. Ascorbic acid can be depleted from the medium under pseudo-first-order conditions and expressed in the following equation:

$$-d[O_2]/dt = k_5[O_2], \quad (24)$$

where

$$k_5 = k_4[\text{AsA}]. \quad (25)$$

[AsA] is considered constant throughout the reaction and can be modified to obtain different k_5 values. This constant (k_5) is linearly dependent on the concentrations of Pt nps (Supporting Fig. 5A, B). In addition, k_6 can be determined from the slope of these plots:

$$\ln \{ [\text{O}_2]_0 / [\text{O}_2] \} / [\text{Pt nps}] = k_6 t, \quad (26)$$

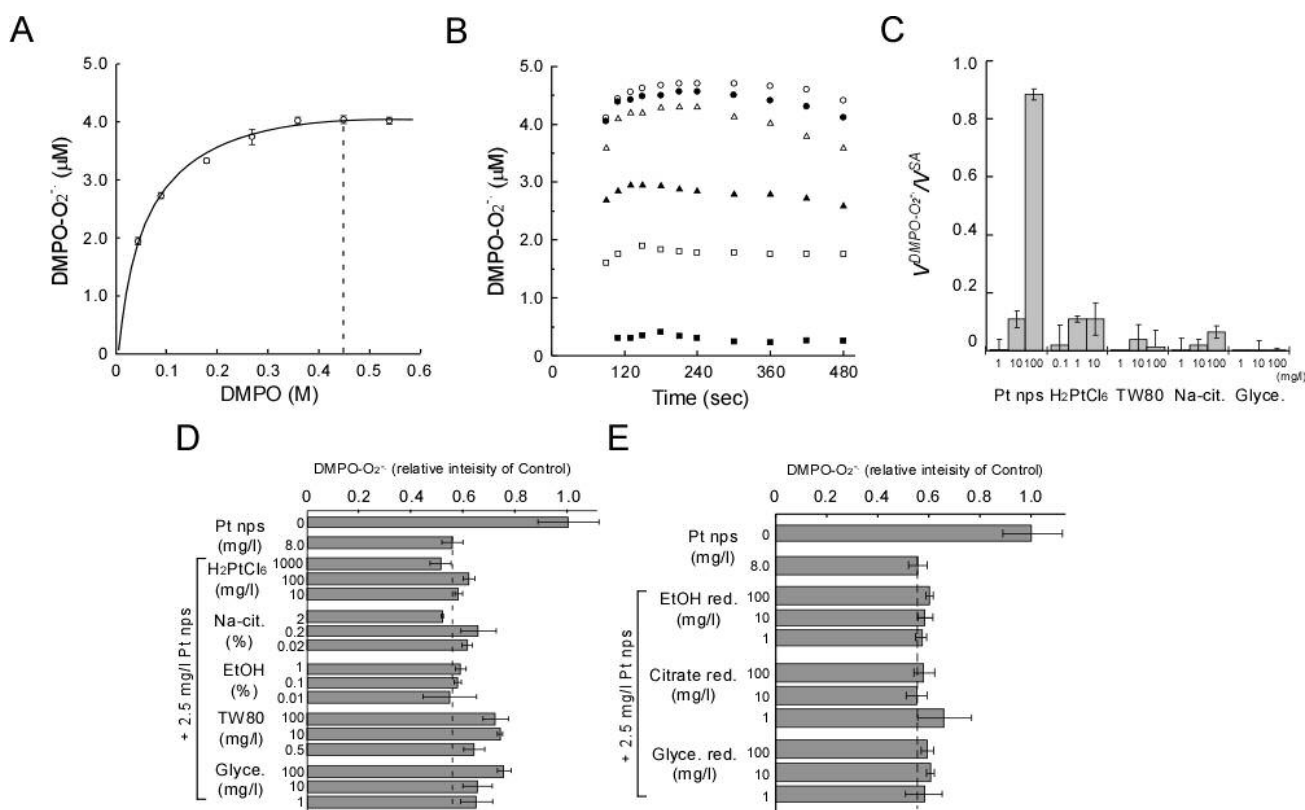
where $[\text{O}_2]$ is the concentration of dissolved oxygen at time (t), $[\text{O}_2]_0$ is the concentration of dissolved oxygen at time zero, and k_6 is a constant value determined from the above plots. The kinetics study was conducted by measuring the consumption of oxygen under pseudo-first-order conditions at 27°C. Determination of k_5 was conducted in triplicate using five different concentrations of Pt nps.

Supporting Table 1. Rate constants for ascorbic acid autoxidation in the presence of Pt nps and contaminating substances.

Added to the Reaction Mixture	$k_6 \times 10^4 / \text{sec}^{-1} \cdot \text{mg}^{-1} \cdot \text{L}$
No addition	
(background autoxidation)	6.10 ± 1.6 (k_5)
1 nm Pt nps	$6.10 \pm 1.1^{*\alpha}$
2 nm Pt nps	10.6 ± 2.1
3 nm Pt nps	$50.1 \pm 5.9^{*\beta}$
3-5 nm Pt nps	11.5 ± 2.6
20 min Agg Pt nps	$20.5 \pm 1.8^{*\square}$
40 min Agg Pt nps	$32.4 \pm 4.2^{*\square}$
60 min Agg Pt nps	$36.6 \pm 3.2^{*\square}$
6 nm Au nps	2.66 ± 2.2
H_2PtCl_6	5.67 ± 2.1
Tween 80	1.27 ± 1.1
Na-citrate	3.88 ± 2.0
Glycerol	1.08 ± 1.0

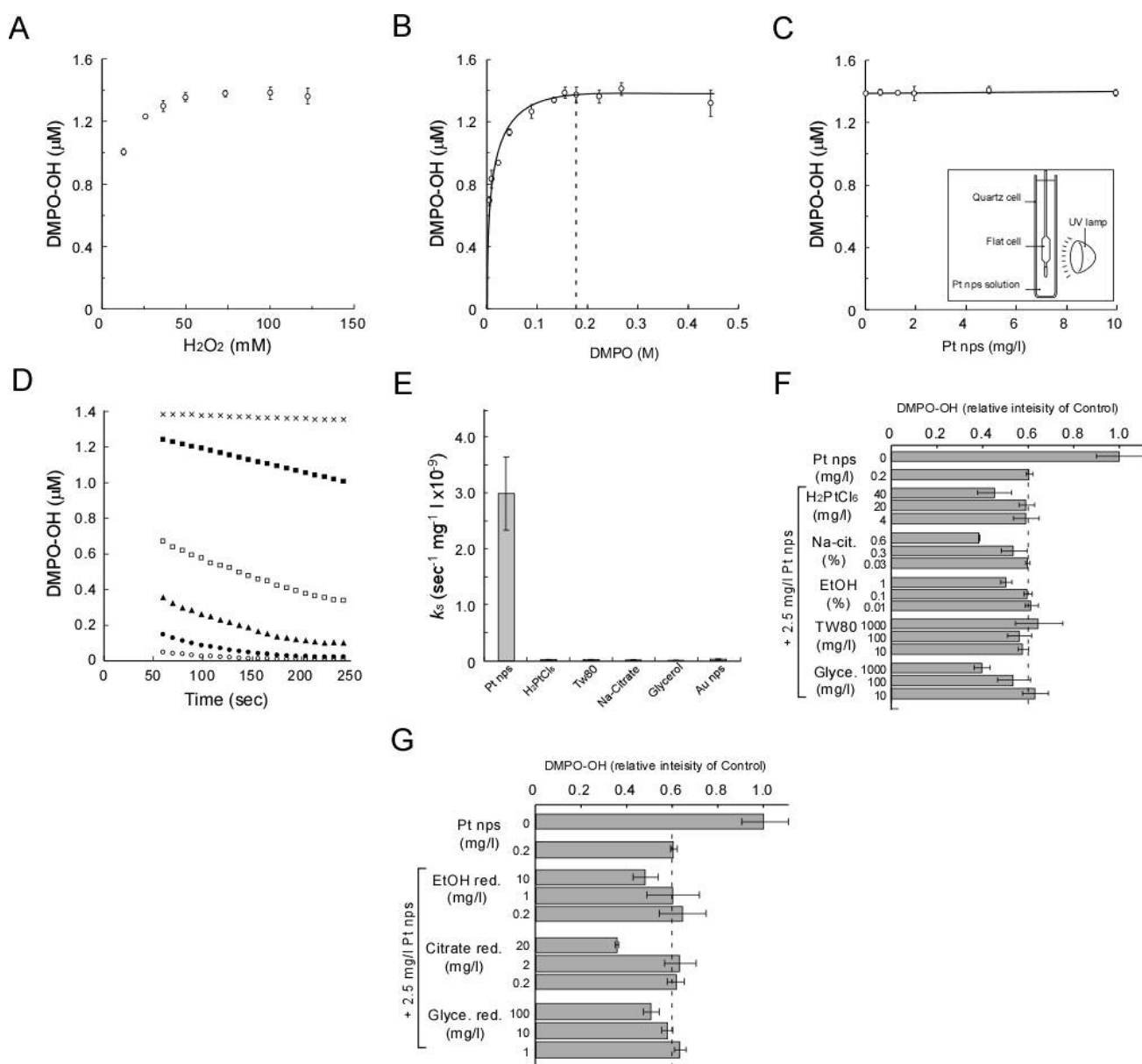
The reaction mixture contained 40 mM sodium phosphate buffer (pH 7.8) and 25 mM ascorbic acid. As materials that might be in the purified Pt nps solution, the effect of 20 mg/L H_2PtCl_6 , 20 mg/L Tween80, 1 mM sodium citrate and 10 mg/L glycerol were examined. Agglutinated nps (Agg Pt nps) were prepared by

autoclaving at 170°C for 20, 40 and 60 min and 5 nm. Asterisks indicate $p < 0.05$ (* α) and $p < 0.01$ (* β) compared with 2 nm Pt nps, respectively.

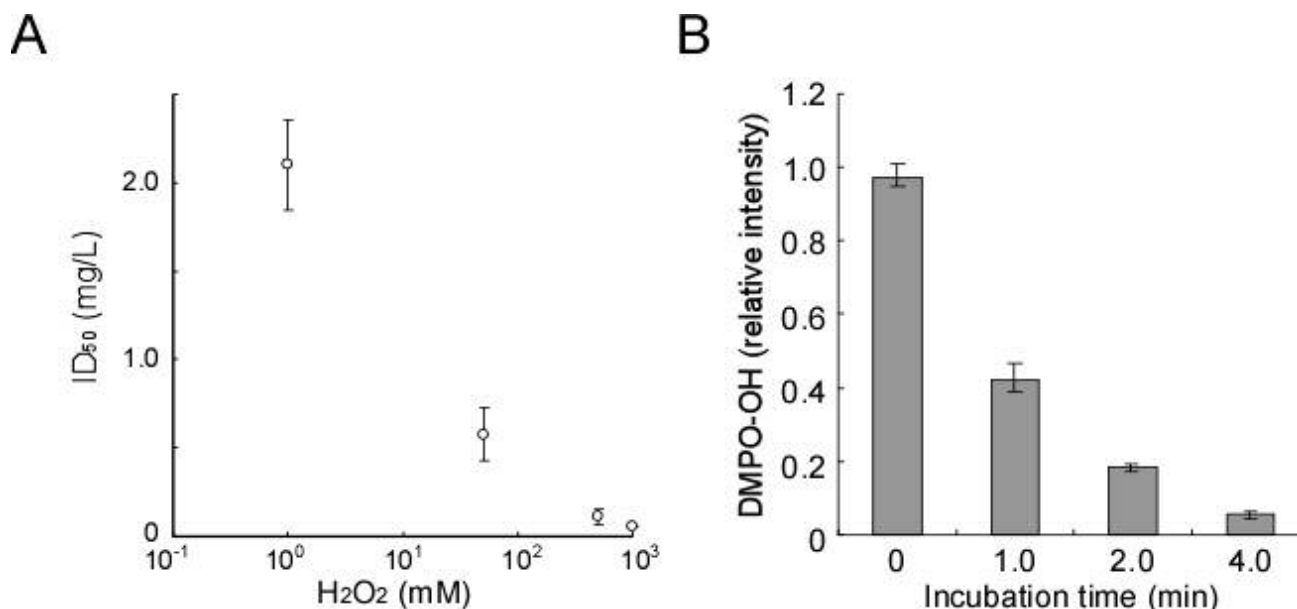


Supporting Fig. 1. Superoxide anion radical ($O_2^{\bullet-}$)-scavenging activity of Pt nps. (A) Concentration of DMPO- $O_2^{\bullet-}$ versus that of DMPO in the HPX-XOD system. Each sample contained 0.2 mM HPX, 100 μ M DETAPAC, 40 mM sodium phosphate buffer (pH 7.4) and 20 U/L of XOD. (B) Levels of DMPO- $O_2^{\bullet-}$ adducts in the presence of Pt nps. Open circles, 0 mg/L of Pt nps; closed circles, 0.1 mg/L; open triangles, 1 mg/L; closed triangles, 5 mg/L; open squares, 20 mg/L; closed squares, 80 mg/L. (C) Influence of the coexisting substances hydrogen hexachloroplatinate (H_2PtCl_6), Tween80 (TW80), sodium citrate (Na-cit.) and glycerol (Glyce.) on DMPO- $O_2^{\bullet-}$ signal intensity. (D) Influence of the coexisting substances hydrogen hexachloroplatinate (H_2PtCl_6), sodium citrate (Na-cit.), ethanol (EtOH), Tween80 (TW80), and glycerol (Glyce.) on DMPO- $O_2^{\bullet-}$ signal intensity present in the Pt nps. (E) Influence of the supernatant from ethanol reduction Pt nps solution (EtOH red.), citrate reduction Pt nps solution (Citrate red.) and glycerol reduction (Glyce. red.) on DMPO- $O_2^{\bullet-}$ signal intensity present in the Pt nps. Each Pt nps solution was ultracentrifuged at 50,000 rpm for 2 h. Supernatant from the ultracentrifuged Pt nps solution was used for the experiments. The presented value of the supernatant solution is the concentration of Pt nps before ultracentrifugation.

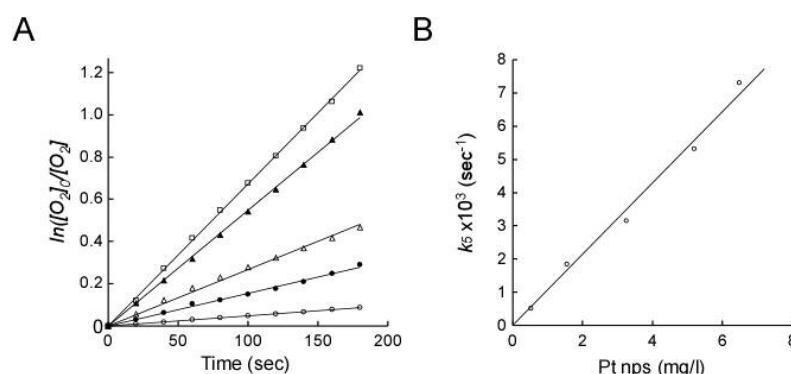
correlation coefficient was 0.995. (C) Hydrogen peroxide concentration-dependence of the initial rate of oxygen production. The values of V_{max} and K_m were $6.04 \mu\text{M O}_2 \text{ sec}^{-1}$ (5.19-6.90: 95 % confidence interval, CI) and 127.8 (97.3-158.3) mM. (D) Effects of Pt nps and coexisting substances on decomposition of hydrogen peroxide. Present where noted were 2 nm Pt nps (Pt nps), 20 mg/L H_2PtCl_6 (H_2PtCl_6), 20 mg/L Tween 80 (Tw80), 1 mM sodium citrate (Na-Citrate) and 10 mg/L glycerol (Glycerol), gold nps (Au nps).



Supporting Fig. 4. Analysis of $\cdot\text{OH}$ scavenging activity of Pt nps. (A) Effect of DMPO- $\cdot\text{OH}$ production by hydrogen peroxide concentration in the Fenton system. (B) Effect of DMPO- $\cdot\text{OH}$ production by DMPO concentration in the Fenton system. (C) Effect of DMPO- $\cdot\text{OH}$ production after inhibiting UV irradiation with Pt nps concentration. (D) Effect of Pt nps on DMPO- $\cdot\text{OH}$. Intensity of DMPO- $\cdot\text{OH}$ adducts in the presence of Pt nps. Open circles, 200 $\mu\text{g/L}$; closed circles, 100 $\mu\text{g/L}$; closed triangles, 50 $\mu\text{g/L}$; open squares, 25 $\mu\text{g/L}$; cross marks, 0 $\mu\text{g/L}$ of Pt nps. (E) Effects of Pt nps and coexisting substances on $\cdot\text{OH}$ -scavenging activity. Where noted, 2 nm Pt nps (Pt nps), 20 mg/L H_2PtCl_6 (H_2PtCl_6), 20 mg/L Tween 80 (Tw80), 1 mM sodium citrate (Na-Citrate) and 10 mg/L glycerol (Glycerol), gold nps (Au nps) were present. (F) Influence of the coexisting substances hydrogen hexachloroplatinate (H_2PtCl_6), sodium citrate (Na-cit.), ethanol (EtOH), Tween80 (TW80), and glycerol (Glyce.) on DMPO- $\text{O}_2^{\cdot-}$ signal intensity present in the Pt nps. (G) Influence of the supernatant from ethanol reduction Pt nps solution (EtOH red.), citrate reduction Pt nps solution (Citrate red.) and glycerol reduction (Glyce. red.) on DMPO- $\text{O}_2^{\cdot-}$ signal intensity present in the Pt nps. Each Pt nps solution was ultracentrifuged at 50,000 rpm for 2 h. Supernatant from the ultracentrifuged Pt nps solution was used for the experiments. The conditions of (F) and (G) were 100 mM DMPO, 100 mM H_2O_2 , 40 mM phosphate buffer (pH 7.4) and 0.2 mg/L Pt nps.



Supporting Fig. 5. (A) Regression plot of ID_{50} versus H_2O_2 concentration. This UV/ H_2O_2 system contains: 178 mM DMPO, 40 mM phosphate buffer (pH 7.4). (B) Regression plot of DMPO-OH adducts incubated with Pt nps. This UV/ H_2O_2 system contains 178 mM DMPO, 100 mM H_2O_2 , 40 mM phosphate buffer (pH 7.4) and 0.2 mg/L Pt nps. We adjusted the UV irradiation to produce DMPO-OH adducts at the same level under all conditions.



Supporting Fig. 6. Oxidation activity of Pt nps. (A) Stimulation of oxygen consumption concomitant with autoxidation of AsA in the presence of Pt nps. Time courses of $\ln([\text{O}_2]_0/[\text{O}_2])$ for the reaction between Pt nps and AsA are shown. The Pt nps concentrations were as follows: open circles, 0.2 mg/L; closed circles, 0.5 mg/L; open triangles, 1.25 mg/L; closed triangles, 2.0 mg/L; and closed squares, 2.5 mg/L. The reactions were started by the addition of different concentrations of Pt nps to a reaction solution containing 25 mM AsA in 40 mM sodium phosphate buffer (pH 7.8) at 27°C. (B) Plot of the rate constant (k_5) for oxygen consumption versus Pt nps concentration. The correlation coefficient was 0.992.

2.1. References

- (1) Mitsuta, K.; Hiramatsu, M.; Ohyanishiguchi, H.; Kamada, H.; Fujii, K. *Bull. Chem. Soc. Jpn.* **1994**, *67*, 529-538.
- (2) Mitsuta, K.; Mizuta, Y.; Kohno, M.; Hiramatsu, M.; Mori, A. *Bull. Chem. Soc. Jpn.* **1990**, *63*, 187-191.
- (3) Finkelstein, E.; Rosen, G. M.; Rauckman, E. J. *J. Am. Chem. Soc.* **1980**, *102*, 4994-4999.
- (4) Hernandez-Ruiz, J.; Arnao, M. B.; Hiner, A. N. P.; Garcia-Canovas, F.; Acosta, M. *Biochem. J.* **2001**, *354*, 107-114.
- (5) Carpenter, J. H. *Limnol Oceanogr.* **1966**, *11*, 264-277.
- (6) Naito, Y.; Yoshikawa, T.; Tanigawa, T.; Sakurai, K.; Yamasaki, K.; Uchida, M.; Kondo, M. *Free*

Radic. Biol. Med. **1995**, 18, 117-123.

(7) Einschlag, F. S. G.; Carlos, L.; Capparelli, A. L. *Chemosphere* **2003**, 53, 1-7.